

## THE INFRARED THERMAL WAVE IMAGING DETECTION OF MICRO-CRACK DEFECTS IN Ti-AL ALLOY PLATE

by

**Chiwu BU<sup>a\*</sup>, Xibin ZHANG<sup>a</sup>, Guozeng LIU<sup>a</sup>,  
Qingju TANG<sup>b</sup>, and Zugen YAN<sup>a</sup>**

<sup>a</sup> College of Light Industry, Harbin University of Commerce, Harbin, China

<sup>b</sup> School of Mechanical Engineering, Heilongjiang University of Science and Technology,  
Harbin, China

Original scientific paper

<https://doi.org/10.2298/TSCI180909227B>

*The Ti-Al alloy has good physical, chemical and mechanical properties, and it is the preferred material in aerospace and other special fields. The laser spots array is used for thermal excitation of the Ti-Al alloy specimen. Based on the fractional differential equation and Fourier heat conduction equation, the fractional heat transfer model of Ti-Al alloy plate specimen excited by short pulse laser spots array is established, and the infrared thermal imaging simulation analysis is carried out by finite element method. The effects of crack width, crack depth and the distance between the crack and its nearest laser spot center on temperature abrupt jump is analyzed. With the increase of crack width and depth, the temperature abrupt jump increases, but the trend gradually slows down. The distance between the crack and its nearest laser spot center has a significant effect on the temperature abrupt jump. With the increase of the distance, the temperature abrupt jump first increases and then decreases. When the distance equals the laser spot radius, that is, the crack is tangent to the spot, the temperature abrupt jump reaches its maximum.*

Key words: *Ti-Al alloy, micro-crack, fractional differential, infrared thermal imaging*

### Introduction

The Ti-Al alloy is one of the lightweight super alloy materials with the best comprehensive properties, and is the preferred material for aerospace engine, supersonic aircraft, and nuclear power plant. The Ti-Al alloys need to undergo laser melting, metallurgical reaction, hot isostatic pressing, isothermal forging, mechanical processing, and other processes in production and engineering applications. The existence of voids and impurities will inevitably lead to structural defects of the material itself, and the internal cracks of the material will occur. In addition, Ti-Al alloy parts in high temperature, high pressure, high load and other complex working environment, also lead to produce internal or surface micro-cracks. The cracks will degrade the comprehensive properties and even cause the occurrence of safety accidents. Therefore, it is necessary to carry out non-destructive testing (NDT) for micro cracks in Ti-Al alloy to take suitable NDT procedures for the quality check and health monitoring of Ti-Al alloy structures. Ultrasonic set-ups are usually used for post-manufacturing quality check. Ultrasonic pulse echo, ultrasonic phased array and eddy current testing are effective in detecting small

\* Corresponding author, e-mail: buchiwu@126.com

cracks, pores and delamination, but they are just suitable for small parts of the analysis, and are not convenient for large areas of analysis [1-3]. Transient thermal imaging technology is a popular accepted technique for large area detection can be done quickly and without contact, and because real images of defects can be easily recorded and analyzed in [4-7]. Infrared NDT has been widely used in aerospace, nuclear power, petrochemical industry due to its non-contact, high efficiency, simple operation and no coupling [8-10]. Infrared thermal wave non-destructive detection is mainly divided into pulsed infrared thermal imaging [11], phase-locked thermal imaging [12], ultrasonic thermal imaging [13]. Pulsed infrared thermal imaging has become mature with high detection efficiency and wide application range. The main aims of the manuscript is to establish the fractional heat transfer model of Ti-Al alloy plate specimen excited by short pulse laser spots array and to be carried out the infrared thermal imaging simulation analysis by the finite element method.

### Detection principle

Under the action of external heat source, the temperature of Ti-Al alloy specimen rises, and the temperature field distribution tends to change gradually from heat source to infinite area. Due to the existence of cracks in the material itself, the heat transfer leads to temperature abrupt jump on both sides of the crack. According to Fourier heat equation, the heat conduction equation of Ti-Al alloy plate under short pulse Gauss laser excitation can be expressed [14]:

$$\frac{\partial T}{\partial t} = \frac{\lambda}{\rho C_p} \frac{\partial^2 T}{\partial x^2} \quad (1)$$

where  $T$  is the temperature distribution,  $\rho$  – the material density,  $C_p$  – the specific heat capacity,  $t$  – the time,  $x$  – the thermal conduction distance, and  $\lambda$  – the thermal conductivity coefficient.

The fractional order heat transfer parameter model was given [15]:

$$\rho C_p \frac{\partial T}{\partial t} + \rho C_p \frac{\Delta t^\alpha}{\Gamma(\alpha+1)} \frac{\partial^{\alpha+1} T}{\partial t^{\alpha+1}} + \nabla q = Q + Q_{ea} \quad (2)$$

$$q = -k \nabla T \quad (3)$$

$$k = \frac{\lambda}{\rho C_p} \quad (4)$$

where  $\rho$  is the material density,  $C_p$  – the specific heat capacity,  $\lambda$  is the thermal conductivity coefficient,  $Q$  – the heat of outflow,  $Q_{ea}$  – the absorbed heat. The space of the crack is defined as air. The thermo-physical parameters of the material are shown in tab. 1.

**Table 1. Thermal physical properties parameters**

Material	Density [kgm <sup>-3</sup> ]	Specific heat capacity [Jkg <sup>-1</sup> °C <sup>-1</sup> ]	Thermal conductivity coefficient [Wm <sup>-1</sup> k <sup>-1</sup> ]
Ti-6Al-4V	4500	612	15.24
Air	1.29	1000	0.024

### Experimental study

#### Sample preparation and experimental methods

Gauss pulse laser with thermal power  $P = 1000$  kW is taken as the excitation source. The laser beam is divided into  $5 \times 5$  array laser spots with the diameter of  $D = 3$  mm, and a

Ti-Al alloy thin plate of 60 mm × 60 mm × 6 mm is used as the simulation specimen. The position distribution of the laser spots array on the surface of the specimen is shown in fig. 1. The Gauss impulse function  $G(t)$  can be written:

$$G(t) = e^{-\frac{(t-0.1)^2}{0.4}} \quad (5)$$

The distance between the crack and its nearest laser spot center is  $l$ , as shown in fig. 2. The surface temperature abrupt jump between the two sides of the crack symbolled  $\Delta T$  is the used to analyze the effect of the width and depth of the crack, and the distance between the crack and its nearest laser spot center.

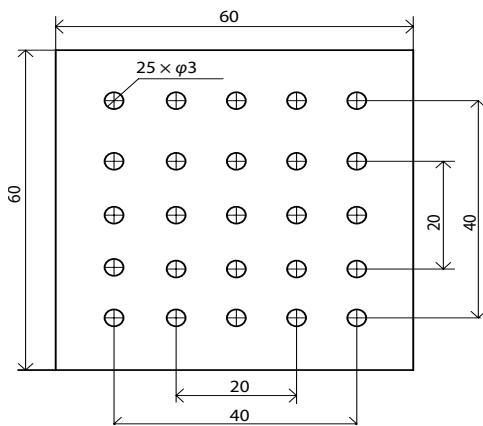


Figure 1. Laser spots distribution

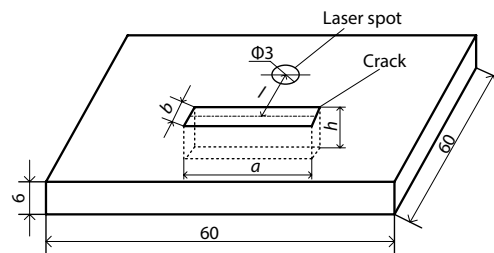


Figure 2. Scheme of crack inside the specimen

### Numerical simulation and results analysis

The temperature distribution of the upper surface of Ti-Al alloy under thermal excitation can be obtained by the finite element simulation calculation. The factors affecting the temperature distribution include the thermal conductivity of the specimen, the power of the excitation source, the time of simulation calculation, the geometric parameters of the crack and the location of the crack. Figure 3 shows the upper surface temperature distribution of transversal line cross the crack defect location. From fig. 3, it can be seen that the temperature curve is smooth Gaussian curve at the crack-free zone. While the temperature curve has an abrupt jump at the crack zone.

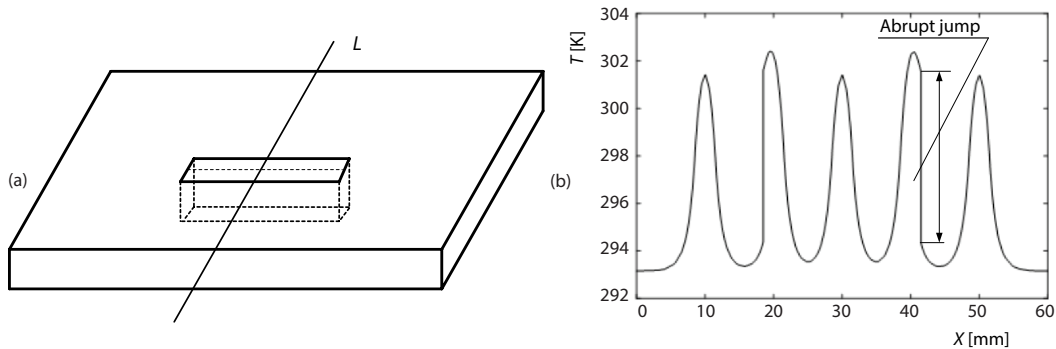


Figure 3. Upper surface temperature distribution of transversal line cross the defect location; (a) the transversal line (b) temperature distribution of transversal line

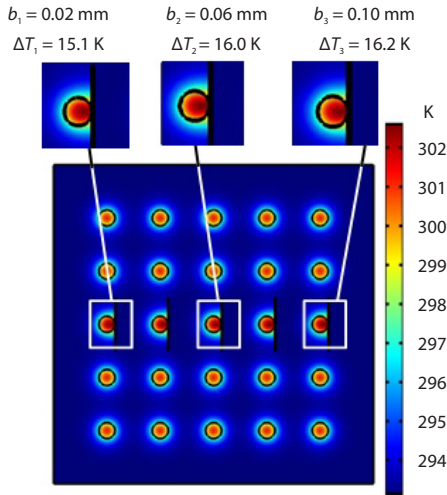


Figure 4. The temperature distribution of the specimen surface with different crack width

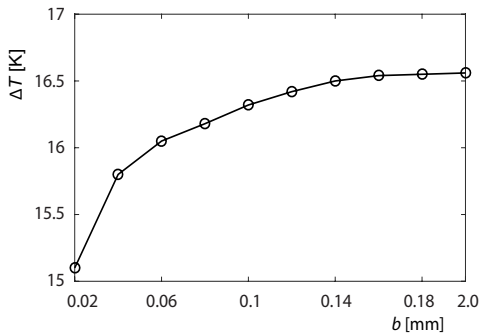


Figure 5. The effect of crack width,  $b$ , to temperature abrupt jump ( $a = 10$  mm,  $h = 5$  mm)

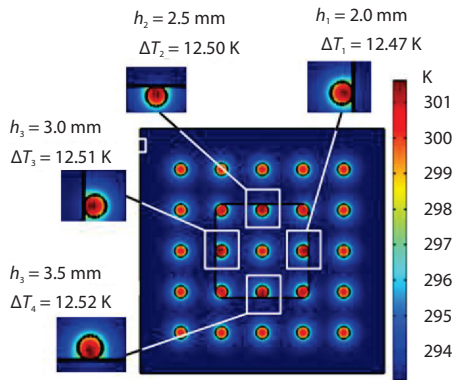


Figure 6. The temperature distribution of the specimen surface with different crack depth

*The effect of crack width,  $b$ , to temperature abrupt jump*

Figure 4 shows the upper surface temperature distribution of specimens with crack length  $a = 10$  mm, crack depth  $h = 5$  mm, crack distance  $l = 3$  mm, and crack width  $b = 0.02$  mm,  $0.06$  mm, and  $0.10$  mm, respectively. The temperature abrupt jumps  $\Delta T = 15.1$  K,  $16.0$  K, and  $16.2$  K, respectively. It can be seen that the crack width has a significant effect on the upper surface temperature abrupt jumps of specimen with cracks. In order to obtain the effect of crack width on temperature abrupt jump, more different crack widths, such as temperature abrupt jumps corresponding to the widths  $0.04$ ,  $0.08$ ,  $0.12$ ,  $0.14$ ,  $0.16$ ,  $0.18$ , and  $0.20$ , are also simulated and calculated under the premise that the length and depth of the cracks remain unchanged. Thus, the effect of crack width on temperature abrupt jump is obtained, as shown in fig. 5.

Figure 5 shows that when the crack width is in the range of  $0-0.14$  mm, the temperature abrupt jump at the crack zone is larger. When the crack width is in the range of  $0.14-0.2$  mm, the change range is smaller, it means that, with the increase of crack width, it has less and less effect on temperature abrupt jump.

Figure 6 shows the upper surface temperature distribution of specimen with crack length  $a = 20$  mm, crack width  $b = 5$  mm, distance  $l = 3$  mm and crack depth  $h = 2.0$  mm,  $2.5$  mm,  $3.0$  mm, and  $3.5$  mm, respectively. The temperature abrupt jump  $\Delta T = 12.47$  K,  $12.50$  K,  $12.51$  K, and  $12.52$  K, respectively. It can be seen that the crack depth has an obvious effect on the upper surface temperature abrupt jumps of specimen with cracks. In order to obtain the effect of crack depth on temperature abrupt jump, more different crack depths, such as temperature abrupt jumps corresponding to  $4$ ,  $4.5$ ,  $5$ , and  $5.5$  mm, are also simulated and calculated under the premise that the length and width of the cracks remain unchanged. Thus, the effect of crack depth on temperature abrupt jump is obtained, as shown in fig. 7.

Figure 7 shows that, with the increase of crack depth, the change of temperature jump tends to be stable.

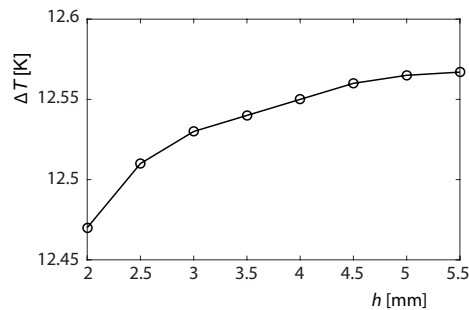
*Effect of crack position on temperature jump*

Figure 8 shows the upper surface temperature distribution of specimen with crack length  $a = 5$  mm, crack width  $b = 0.01$  mm, crack depth  $h = 5$  mm and the distance between the crack and its nearest laser spot center  $l = 0.75$  mm, 1.5 mm, and 3.0 mm, respectively. The temperature abrupt jumps  $\Delta T = 2.78$  K, 14.3 K, and 0.57 K, respectively. It can be seen that the distance has a significant effect on the upper surface temperature abrupt jumps of specimen with cracks. In order to obtain the effect of the distance on temperature abrupt jump, more different distance values, such as temperature abrupt jumps corresponding to 0.25 mm, 0.5 mm, 1 mm, 1.25 mm, 2 mm, 2.5 mm, 4 mm, 4.5 mm, and 5.0 mm, are also simulated and calculated under the premise that the length and width of the cracks remain unchanged. Thus, the effect of the distance between the crack and its nearest laser spot center on temperature abrupt jump is obtained, as shown in fig. 9.

Figure 9 shows that when the distance  $l = 0-1.5$  mm, *i. e.*, the crack intersects with the laser spot, with the increase of  $l$ , the temperature abrupt jump  $\Delta T$  also increases. When the distance  $l = 1.5-5.0$  mm, *i. e.*, the crack is separated from the laser spot, as the distance  $l$  increases, the temperature abrupt jump  $\Delta T$  becomes smaller and smaller. When the distance  $l = 1.5$  mm, the crack is tangent to the laser spot, the temperature abrupt jump  $\Delta T$  reaches the maximum. When the distance  $l = 5$  mm, the crack is located at the middle of the two laser spots, and the temperature abrupt jump  $\Delta T$  is almost zero.

**Conclusion**

The infrared thermal imaging simulation model based on fractional heat transfer theory was used to calculate the temperature distribution on the surface of Ti-Al alloy plate specimen under thermal excitation of laser spots array. The existence of cracks in the specimen leads to surface temperature abrupt jump. The effects of crack width, crack depth and the distance between the crack and its nearest laser spot center on temperature abrupt jump is analyzed. With the increase of crack width and depth, the temperature abrupt jump increases, but the trend gradually slows down. The distance between the crack and its nearest laser spot center has a significant effect on the temperature abrupt jump. With the increase of the distance, the temperature abrupt jump first



**Figure 7. The effect of crack depth,  $h$ , to temperature abrupt jump ( $a = 20$  mm,  $b = 5$  mm,  $l = 3$  mm)**

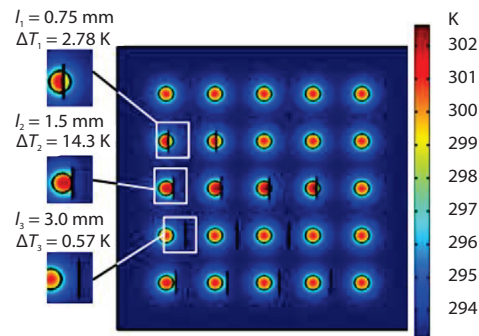


**Figure 8. Surface temperature distribution of specimen under different crack locations**

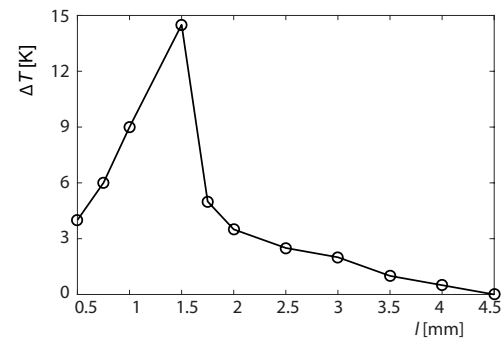


**Figure 9. Effect of crack position on temperature abrupt jump ( $a = 5$  mm,  $b = 0.01$  mm,  $h = 5$  mm)**

increases and then decreases. When the distance equals the laser spot radius, that is, the crack is tangent to the spot, the temperature abrupt jump reaches its maximum.

### Acknowledgment

This project is supported by National Natural Science Foundation of China (Grant No. 51775175), Harbin University of Commerce Youth Innovative Talents Support Project (Grant No. 2016QN066), Heilongjiang Province Natural Science Fund (Grant No. E2018050), Harbin Innovation Fund Project for Talent Youth (Grant No. 2013RFQXJ089).

### Nomenclature

$C_p$  – specific heat capacity, [ $\text{Jkg}^{-1}\text{K}^{-1}$ ]  
 $Q$  – heat of outflow, [J]  
 $Q_{ca}$  – absorbed heat, [J]  
 $T$  – temperature distribution, [K]  
 $t$  – time, [s]

$x$  – thermal conduction distance, [m]

#### Greek symbols

$\lambda$  – thermal conductivity coefficient, [ $\text{Wm}^{-1}\text{k}^{-1}$ ]  
 $\rho$  – material density, [ $\text{kgm}^{-3}$ ]

### References

- [1] Sinke, J., Some Inspection Methods for Quality Control and In-Service Inspection of GLARE, *Applied Composite Materials*, 10 (2003), 4-5, pp. 277-291
- [2] Bonavolonta, et al., Eddy Current Technique Based on -SQUID and GMR Sensors for Non-Destructive Evaluation of Fiber/Metal Laminates, *IEEE Transactions on Applied Superconductivity*, 19 (2009), 3, pp. 808-811
- [3] Satyanarayan, L., et al., Simulation of Ultrasonic Phased Array Technique for Imaging and Sizing of Defects Using Longitudinal Waves, *International Journal of Pressure Vessels and Piping*, 84 (2007), 12, pp. 716-729
- [4] Wang, F., et al., Experimental Study on GFRP Surface Cracks Detection Using Truncated-Correlation Photo-Thermal Coherence Tomography, *International Journal of Thermophysics*, 39 (2018), 4, 49
- [5] Zhang, H., et al., Optical Excitation Thermography for Twill / Plain Weaves and Stitched Fabric Dry Carbon Fibre Preform Inspection, *Composites – Part A: Applied Science and Manufacturing*, 107 (2018), Apr., pp. 282-293
- [6] Zhang, H., et al., An Experimental and Analytical Study of Micro-Laser Line Thermography on Micro-Sized Flaws in Stitched Carbon Fiber Reinforced Polymer Composites, *Composites Science and Technology*, 126 (2016), Apr., pp. 17-26
- [7] Wang, F., et al., Research on Debonding Defects in Thermal Barrier Coatings Structure by Thermal-Wave Radar Imaging (TWRI), *International Journal of Thermophysics*, 39 (2018), 6, 71
- [8] Wang, Y., et al., Thermal Pattern Contrast Diagnostic of Micro Cracks with Induction Thermography for Aircraft Braking Components, *The IEEE Transactions on Industrial Informatics*, 14 (2018), 12, 1
- [9] Bittinat, D. C., et al., Defect Detection in Fuel Cell Gas Diffusion Electrodes Using Infrared Thermography, *The ECS Transactions*, 58 (2013), 1, pp. 495-503
- [10] Schuss, C., et al., Defect Localisation in Photo-Voltaic Panels With the Help of Synchronized Thermography, *Proceedings, Instrumentation and Measurement Technology Conference, Turin, Italy, 2017*
- [11] Ishikawa, et al., Detecting Deeper Defects Using Pulse Phase Thermography, *Infrared Physics and Technology*, 57 (2013), 57, pp. 42-49
- [12] Razani, M., et al., Lock-in Thermography Using a Cellphone Attachment Infrared Camera, *Aip Advances*, 8 (2018), 3, 035305
- [13] Palumbo, D., et al., Ultrasonic Analysis and Lock-in Thermography for Debonding Evaluation of Composite Adhesive Joints, *Ndt and E International*, 78 (2016), 3, pp. 1-9
- [14] Ezzat, M. A., et al., Two-Temperature Theory in Magneto-Thermoelasticity with Fractional Order Dual-Phase-Lag Heat Transfer, *Nuclear Engineering and Design*, 252 (2012), Nov., pp. 267-277
- [15] Ghazizadeh, H. R., et al., An Inverse Problem to Estimate Relaxation Parameter and Order of Fractionality in Fractional Single-Phase-Lag Heat Equation, *International Journal of Heat and Mass Transfer*, 55 (2012), 7-8, pp. 2095-2101